

**COMPUTER SIMULATION STUDY OF HIGH-PRESSURE GAS QUENCHING  
OF A STEEL ELEMENT WITHIN VACUUM FURNACE BATCH  
FOR DIFFERENT WORKING CONDITIONS**

Fodemski T.R.\* and Jasiński P.  
\*Author for correspondence  
Department of Heat Technology and Refrigeration,  
Technical University of Łódź,  
90-924 Łódź, ul. Stefanowskiego 1/15,  
Poland,  
E-mail: fodemski@p.lodz.pl

**ABSTRACT**

The paper presents analysis of the high-pressure gas quenching of metal elements, after their vacuum carbonisation process, based on the computer simulation. The ANSYS-CFX code has been used for this purpose. This transient quenching process includes challenging problems, which requires deep knowledge and application of heat transfer, fluid mechanics and thermodynamics. The numerical simulation analysis method focuses on a single element contained in an elementary, repeatable section (usually a cuboid) of the whole batch. In this study quenching of a steel cylinder of diameter  $d = 20\text{mm}$  and length  $L = 150\text{ mm}$  is analysed. This approach allows defining precisely: (i) the geometries of the metal element and of the elementary cubical section associated with it and, also, (ii) flow and thermal boundary conditions on the walls of this elementary section. Above definition of the elementary section (a computing domain) allows using the whole available computing power for the quenching process simulation in it. The ratio of volumes mentioned in (i) defines a “porosity of batch” and the analysis covers the range from 7 to 70%. The number of grid points used for the elementary section varies from 55000 to 240000. The influence of the pressure gradient value (a flow “driving force” through the elementary section) and its direction – on temperature and quenching rate time distributions in a steel element – is analysed and presented. The use of periodicity and symmetry conditions, for the velocity field, on the elementary section walls, allows simulating different single element quenching conditions – reflecting its position in the batch. The transient quenching has been usually analysed for a fixed velocity field. However, the steel element body thermal properties in this transient process varied – appropriately to its time dependent temperature distribution. The initial element temperature is assumed to be equal 1300 K. The influence of different gases, i.e. argon, helium, nitrogen

and hydrogen, and their static pressures (up to 30 bar), on the steel element quenching process, is analysed and presented.

**NOMENCLATURE**

$A$	[m]	Distance between cylinder outer walls in the $r$ direction
$d$	[m]	Cylinder diameter
$H$	[m]	Distance between cylinders along the $z$ direction
$L$	[m]	Length of cylinder
$n$	[-]	Number of cylinders
$p$	[bar]	Cooling gas pressure
$\Delta p$	[Pa]	Pressure difference
$dp/dx$	[Pa/m]	Pressure gradient component
$q$	[W/m <sup>2</sup> ]	Heat flux density
$r^*$	[-]	Dimensionless radius
$R$	[m]	Cylinder radius
$t$	[s]	Time
$T$	[K]	Temperature
$w$	[m/s]	Velocity
$x, y, z$	[m]	Cartesian axis direction
$r, \theta, z$	[m]	Cylindrical axis direction
Special characters		
$\alpha$	[W/m <sup>2</sup> K]	Heat transfer coefficient
$\beta$	[-]	Roots of equation
$\lambda$	[W/mK]	Thermal conductivity
$\varepsilon$	[-]	Porosity of the batch
$\rho$	[kg/m <sup>3</sup> ]	Density
$\zeta$	[-]	Friction factor
$g^*$	[-]	Dimensionless temperature
$J_0$	[-]	Bessel function of zero order
$J_1$	[-]	Bessel function of first order
Dimensionless numbers		
$Bi$	[-]	The Biot number
$ Fo$	[-]	The Fourier number
$ Re$	[-]	The Reynolds number

## INTRODUCTION

Vacuum furnaces for high pressure gas quenching have been used for almost thirty years. They have become increasingly favoured for hardening required thickness of some high strength steel elements (shown, for example, in Fig. 1). The quenching technology have progressed in recent years from furnaces with nitrogen at a pressure of 5 bars to systems with hydrogen and hydrogen-nitrogen mixtures at pressures up to 20 bars or with helium at pressures up to 40 bars. These lead to gas quenching intensities more attractive than those achieved with hot quenching oils.



**Figure 1.** Different steel elements after high-pressure gas quenching.

The gas flow through the furnace-quenching loop is caused by a blower (see Fig. 2a). The cooling effect of its load occurs primarily by forced convective heat transfer at the elements surfaces. The driving force of this effect is the temperature difference between the hot element outer surfaces and the flowing gas. Because the temperature field in this process is strongly dependent on the flow field – it must be precisely determined to ensure an accurate prediction of the real temperature time history of the whole volume element during

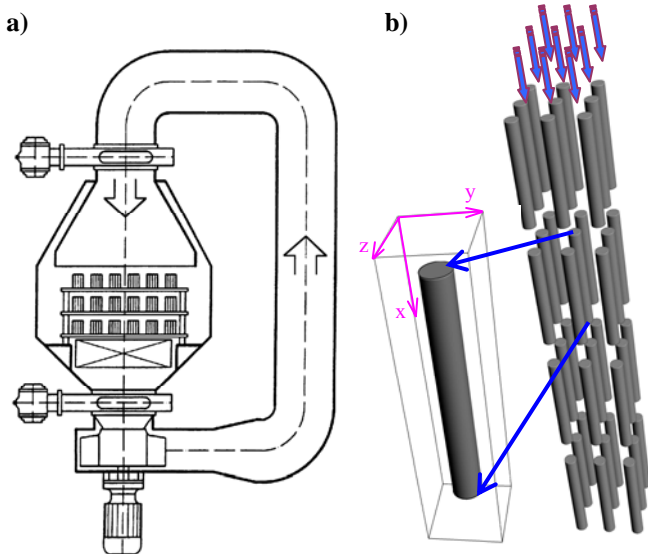


**Figure 2.** The quenching loop (a) and the batch structure (b).

quenching. The hardening response of the parts depends upon many factors which influence heat transfer (quenching) intensity. Among them there are following parameters related to the batch, i.e. (i) weight; (ii) shape and size of the parts, and (iii) the batch design.

## PARAMETERS OF THE BATCH

In this study it is assumed that the furnace batch consists of many cylindrical elements. The study presented in this work focuses on the gas flow and the heat transfer in the cubical elementary section of the batch – as shown in Fig. 2a. The computer code ANSYS-CFX has been used to simulate flow and velocity fields in this section.

When considering a batch, the influence of the following parameters on the velocity field and on the heat transfer in the section have been analysed (see Fig. 3): (i) the axial spacing  $H$  and (ii) the radial spacing  $A$ . The simulations have been made for the cylinder diameter  $d = 20\text{mm}$  and length  $L = 150\text{mm}$  and for combination of the axial and radial spacing values presented in Table 1.

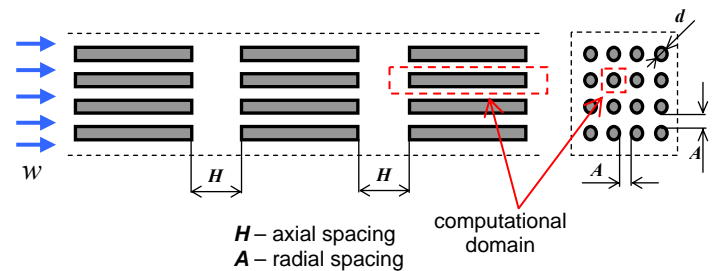


**Figure 3.** The batch structure parameters

**Table 1**

$H$ [mm]	150	100	80	60	40	20	10
$A$ [mm]	60	50	40	30	20	10	

The comparison of the maximum and minimum volumes of the elementary section, i.e. computational domains in the simulations, is shown in Fig. 4. The number of grid points in the elementary section varies from 55000 to 240000. The “batch porosity” values analysed in the computer simulation cover the range from 7 to 70%.

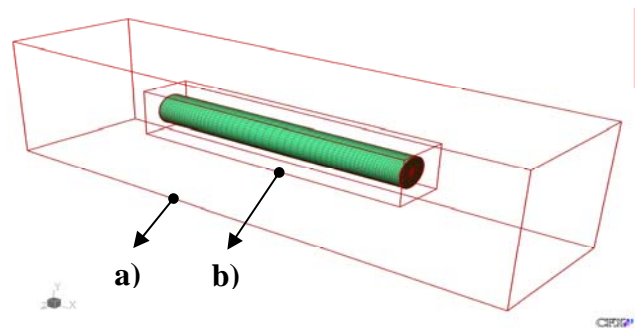


**Figure 4.** The comparison of the maximal (a) and minimal (b) batch elementary section sizes (computational domains).

## VALIDATION OF THE ANSYS-CFX CODE

The validation of simulation results must be carried out for any code, not only for the ANSYS-CFX. This procedure allows setting up values relevant for particular simulation case results accuracy. The most important ones take account of the analyzed heat transfer and flow types and its geometry, i.e.:

- unsteady heat transfer;
- turbulence model and
- mesh size.

The validation procedure adopted in the present work had, in fact, two stages. In both the solid cylinder length  $L \gg d$  was assumed.

The first stage concentrated on the validation related to the unsteady heat transfer. Only two quenching cases, described by the Fourier equation, for two different boundary condition sets, i.e. Newton's and Dirichlet's, are shortly described here. The analytical solutions, for both cases, are given in [5] and can be written, respectively, as:

$$\text{and } g^+ = \sum_{i=1}^{\infty} \frac{2 \cdot J_1(\beta_i)}{\beta_i [J_0^2(\beta_i) + J_1^2(\beta_i)]} \cdot J_0(\beta_i \cdot r^+) \cdot \exp(-\beta_i^2 \cdot Fo)$$

$$\text{where } g^+ = \sum_{i=1}^{\infty} \frac{2}{\beta_i \cdot J_1(\beta_i)} \cdot J_0(\beta_i \cdot r^+) \cdot \exp(-\beta_i^2 \cdot Fo)$$

$$g^+ = \frac{T - T_p}{T_0 - T_p} \quad \text{and} \quad r^+ = \frac{r}{R} \quad \text{are dimensionless coordinates}$$

$$\beta_i \quad \text{are the roots of equation} \quad \frac{J_0(\beta)}{J_1(\beta)} = \frac{\beta}{Bi}$$

$Bi$  and  $Fo$  are Biot and Fourier numbers and

$J_0(\beta_i)$  and  $J_1(\beta_i)$  are Bessel functions of zero and first order, respectively.

It is well known that when  $Bi \rightarrow \infty$  the solution for the Newton boundary conditions becomes the one for the Dirichlet conditions. Both cases, for the same geometry and material parameter values, were calculated numerically using the ANSYS-CFX code. Differences between analytical and numerical results were negligible. They were related rather to the number of  $\beta_i$  roots and grid points density. All conclusions resulting from this exercise were very useful in the further simulation work.

The second stage concerned the simulation of the flow around array of parallel cylinders (with their axes on one plane) with pressure gradient being perpendicular to these axes.

The pressure drop  $\Delta p$  and the friction coefficient  $\zeta$  can be predicted by the following formulas, respectively [6]:

$$\Delta p = \zeta \cdot \frac{\rho \cdot w^2}{2} \quad \zeta = (6 + 9 \cdot n_r) \cdot \left(\frac{x}{d}\right)^{-0.23} \cdot Re^{-0.26}$$

where  $n_r$  – the number of cylinders and  
 $x$  – the distance between cylinders.

The comparison of results, predicted and calculated numerically using the ANSYS-CFX code, with the SST (*Shear Stress Transport*) turbulence model [7], is presented in Fig. 5. The good agreement can be clearly seen.

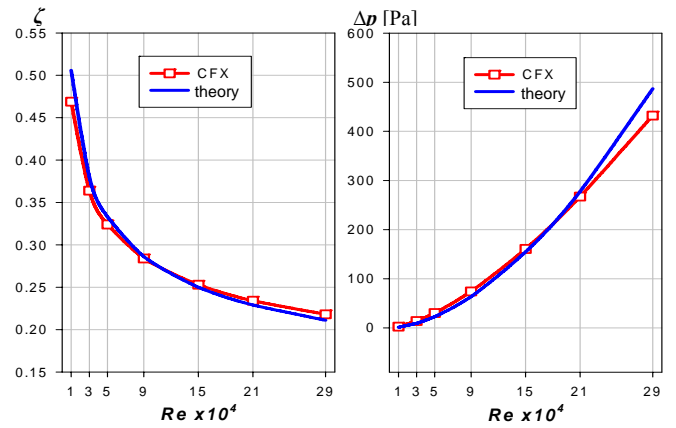


**Figure 5.** Comparison of theoretical [6] and simulation results of the pressure drop and friction coefficient for the cylinder array

## QUENCHING MODEL AND BOUNDARY CONDITIONS

The initial assumption in the model has been made that the velocity field in the elementary section is calculated first – for isothermal conditions. After that it is used to calculate, separately, the element quenching, assuming: (i) forced convection and (ii) neglecting radiation. The assumption (i) is obvious and the second one takes account that in the middle of the batch element is surrounded by other ones which have the same temperature (note also, that the initial surface temperature of elements is 1300 K and drops very rapidly). Since velocity profile at the inlet to this section is determined – it can be always used for simultaneous solution of the velocity and temperature fields in the elementary section. It requires more computing time but allows to progress with the calculation down the flow, even from the first elementary section of the batch (assuming there any velocity profile, for example, a uniform one). It is worth noting, that the most effective work at this stage, from the CPU time point of view, was to perform simulation based on the separate determination of the velocity and temperature fields. More details related to this method are given below.

Specification of the pressure gradient direction and the velocity boundary conditions on all elementary section surfaces is necessary and crucially important to the heat transfer.

It is possible to obtain a "fully developed flow" in the elementary section which is positioned in the middle of the batch rather than at the inlet, outlet or on its sides. In this case one can state that: (i) the pressure gradient direction is aligned with the cylinder axis direction  $x$  (see Figs 2 and 3); (ii) the gas velocity field is periodic in the  $x$ -direction (profiles repeat on inlet and outlet  $z$ - $y$  elementary section surfaces – they are perpendicular to the pressure gradient direction), and (iii) the gas velocity field is symmetrical in  $z$  and  $y$  directions, i.e. all its derivatives are zero on the  $x$ - $z$  and  $x$ - $y$  elementary section side parallel surfaces.

The pressure gradients and the flow velocity fields in elementary sections positioned on the batch sides are different from the patterns at its centre. One can obtain the velocity field differences and distortions related to their position in the batch, and influencing the heat transfer, by the appropriate specification of the boundary conditions. The velocity field in this situation has components in the  $y$  and  $z$  directions. These can be obtained in the elementary section on request that the total pressure

gradient vector has components not aligned with the cylindrical axis  $x$ . In this case there are possible two different sets of the pressure gradient direction and velocity field boundary conditions on the elementary section side surfaces. The first set is: (i) the pressure gradient has a component perpendicular to the  $x$  direction (for simplicity it can be assumed that it has component only in  $x$  or  $y$  direction); (ii) the gas velocity field is symmetric only in the direction where there is no pressure gradient, and (iii) the gas velocity field is periodic in two directions (where there are pressure gradient components). The second set of boundary conditions refers to the case where the pressure gradient is perpendicular to the cylindrical axis  $x$ . This case does not present a practical application in quenching furnaces. However, it has been used for the computer simulation results validation discussed above – for cylinder length  $L \gg d$  – and compared to analytical solutions and reliable experimental data related to the heat transfer and to the pressure drop, respectively.

### COMPUTER SIMULATION QUENCHING RESULTS

Only a sample of quenching results can be presented. All are related to the cylinder made of the 40H steel quenched in the nitrogen. However, the influence of the cooling gas is presented first. In Fig. 6 the mass flow and average velocity through the elementary section, for different gases, are shown, assuming that the pressure gradient forcing the flow has the same value  $dp/dx=350 \text{ Pa/m}$ .

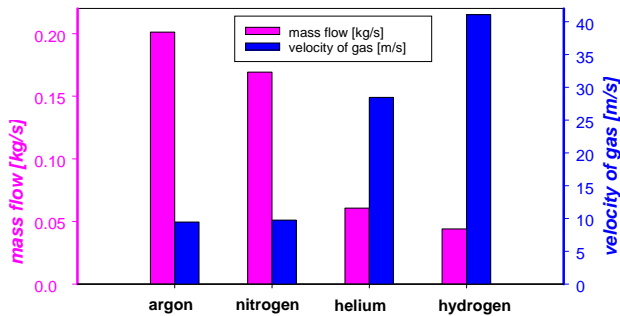


**Figure 6.** Comparison of mass flows and average velocities for different gases; pressure 20 bars and the same pressure gradient

Figs 7 to 9 refer to the time histories of heat transfer quantities related to the quenching by the flow exerted in the elementary section by the pressure gradient aligned with the cylinder axis.

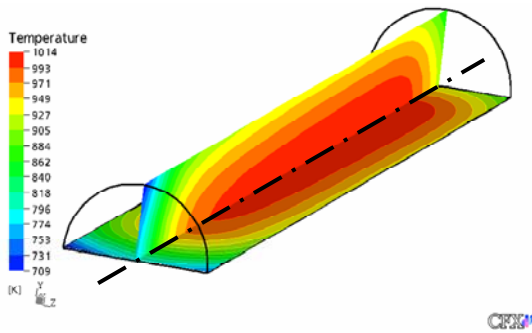


**Figure 7.** Temperature field in the cylinder cross-sections, for  $t=26 \text{ sec}$ , nitrogen at  $p=20 \text{ bar}$

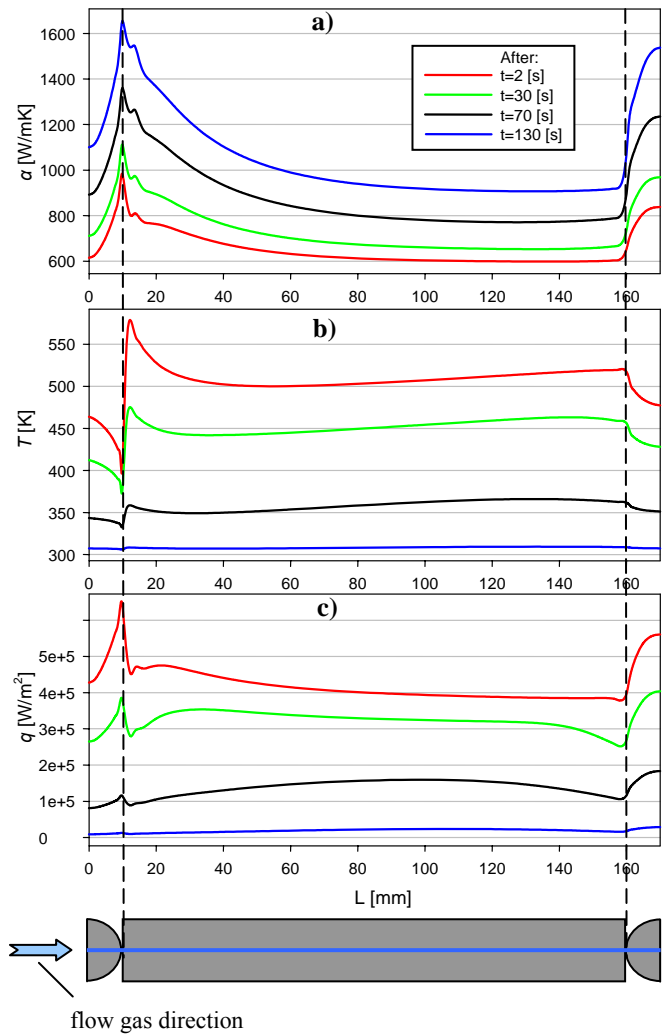


**Figure 8.** Time histories during nitrogen quenching at 20 bars: (a) heat transfer coefficient  $\alpha$ ; (b) temperature profile and (c) surface heat flux

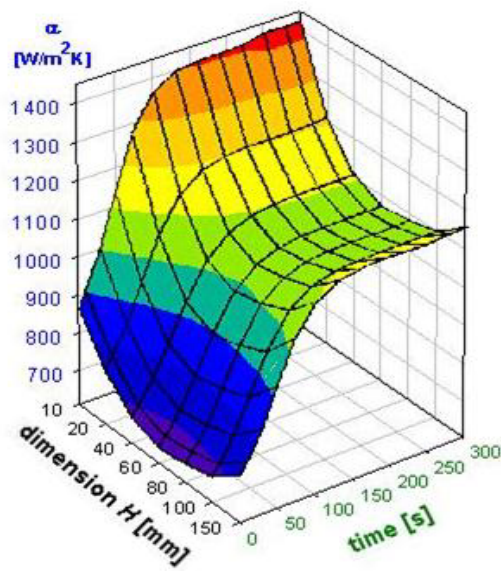


**Figure 9.** The heat transfer coefficient  $\alpha$  time history for range of axial spacing  $H$  values, during nitrogen quenching at 20 bars



Figs 10 to 13 show the differences in similar quantities as presented in Figs 7 to 9 but for the non-axial pressure gradient. Firstly, Fig. 10 presents this angle definition. Figs 11 and 12 show the  $\theta$  value influences on the velocity and temperature fields. The presence of a swirling flow component in Fig. 11 can be clearly seen. This component effect, related to different  $\theta$  values, can be noticed on temperature fields shown in Fig. 12, particularly when confronted with Fig. 7 – where  $\theta=0^\circ$ .

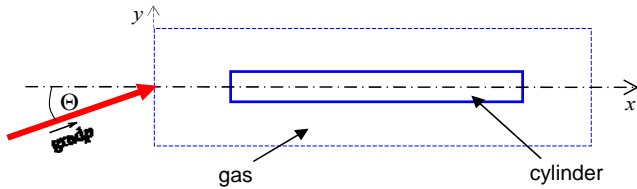


**Figure 10.** Definition of the  $\theta$  angle between the pressure gradient and the cylinder and elementary section symmetry axis.

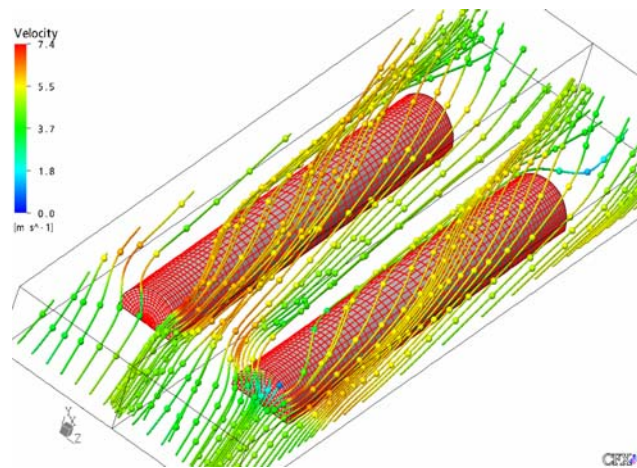


**Figure 11.** The angle  $\theta=30^\circ$  influence on the velocity field in the elementary section:  $A=20\text{ mm}$ ,  $H=60\text{ mm}$  and  $p=20\text{ bar}$

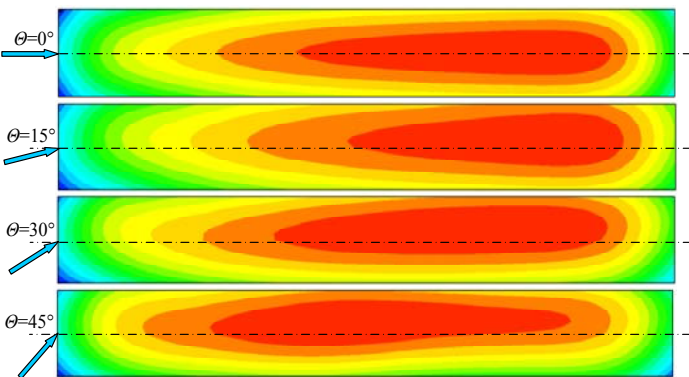


**Figure 12.** The  $\theta$  angle value influence on the temperature field

Finally, Fig. 13 shows the influence of specified  $\theta$  angle values on the element average temperature – as a function of time. Although all curves in Fig. 13a are quite close – the exact value of the difference between average temperatures for axial and non-axial pressure gradients is known from the simulations and

shown in Fig. 13b. It reaches level of about  $35^\circ\text{C}$  and changes with time. It might have negative effects on the hardening process final quality, but precise analysis at this stage is beyond the scope of work.

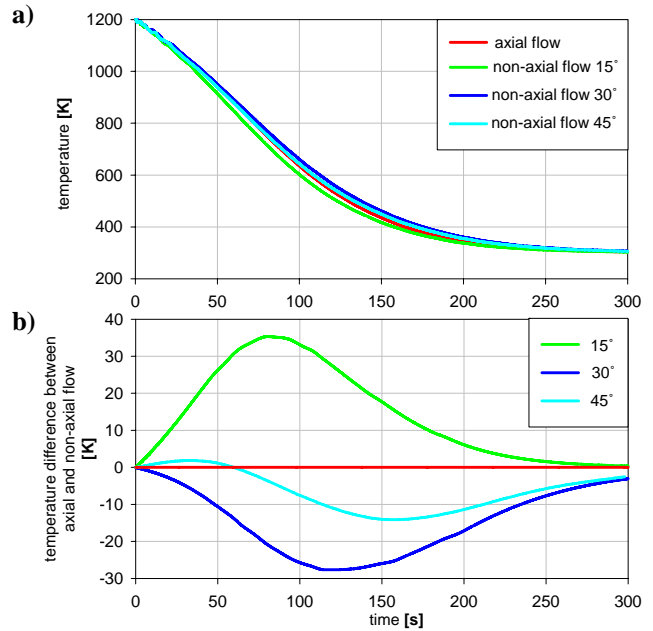


**Figure 13.** The  $\theta$  angle value influence on time history of: (a) the averaged temperature and (b) the averaged temperature difference between the axial flow and non-axial one

### PRACTICAL RESULTS OF SIMULATIONS

The results of the computer simulations give opportunity for deep and thorough analysis. At that stage, the main task was to develop the model. However, apart from a few suggestions already presented in this paper, there are two worth presenting. The first one shown in Fig. 14 is related to the CTP<sub>C</sub>-graph. It allows for material engineering consideration based on quenching parameters from the reliable computer simulation results. This analysis is the next stage of the work.

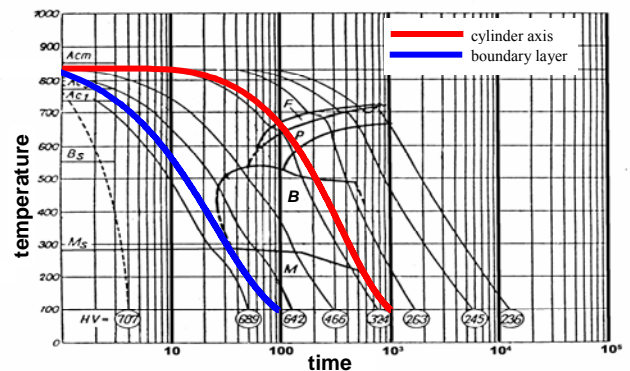


**Figure 14.** The steel 40H CTP<sub>C</sub> graph and quenching curves for: cylinder axis and the surface layer 1mm thick

The other practical result of computer simulation is related to the possibility of new equipment parameter determinations,

including furnaces – predicting data useful for constructors. A small example is given below.

It presents the calculation, based on discussed results of the heat flux time distribution, connected with  $1\text{m}^3$  of the furnace load. Two cases for different batch structures are considered in Figs 15 and 16.

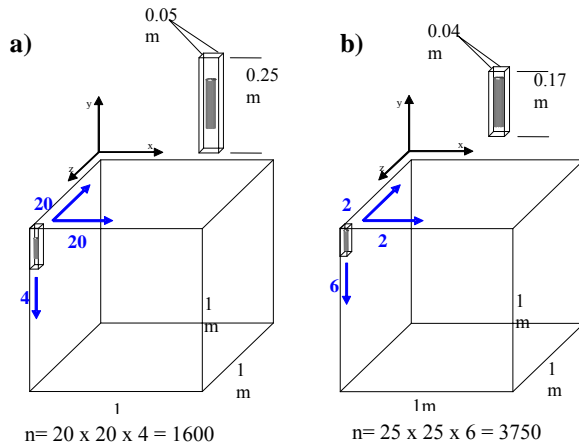


**Figure 15.** Parameters of two batch structures considered;  $n$  – number of elements in the batch

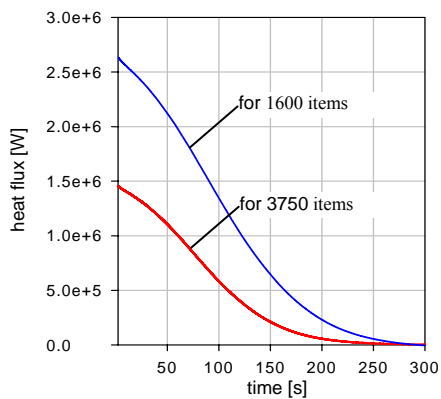


**Figure 16.** The heat flux time distribution extracted from two different batch structures defined in Fig.15.

## CONCLUSION

The presented method of simulation and obtained numerical results compared with the experimental data indicate that this analysis can be used for reliable prediction of the high-pressure transient gas quenching rates after a vacuum carbonisation process. The analysis is focused on a single element of the furnace batch. It allows specifying the gas flow conditions on the elementary cubical section walls associated with this element. They reflect its position in the furnace batch and, therefore, quenching conditions of this element. Although the analysis presented in this work concerns cylinders, the same approach can be used for elements with more complex shapes.

## ACKNOWLEDGMENTS

Authors wish to acknowledge the financial support of the European Community Marie Curie Transfer of Knowledge grant ECHTRA (project No 509847).

## REFERENCES

- [1] Dawes C., Reynoldeon R.W.: Parameters for Gas Quenching In Vacuum Furnaces; *Metal Progress*, July 1971, pp. 72-73;
- [2] Cheary W.J.: Aspects of Vacuum Heat Treatment; *Metallurgy and Metal Forming*, 1973, Vol. 40. No 11, pp. 350-356;
- [3] Bauer E.: Möglichkeiten und Grenzen des Gesabschreckens von Werkzeugstählen in Vakuum-Öfen; *Zeitschrift für wirtschaftliche Fertigung*, 1981, No 8, pp. 405-410;
- [4] Heilman P.: Vacuum Carburizing with Gas Quenching – a New Prospective Technology, *Bul. SECO/WARWICK*, 7, 1999, pp. 7-10;
- [5] Carslaw H. S., Jaeger J. C.: *Conduction of heat in solids*; Oxford University Press, 1959;
- [6] Hobler T.: Ruch ciepła i wymienniki. Inżynieria chemiczna. PWT, Warszawa, 1959;
- [7] AEA Technology plc: CFX-4, *Solver and Solver Manager – User Manual*; CFDS Department, Harwell. UK. Reference Notes, 1999;
- [8] CFX-5, *Solver and Solver Manager – User Manual*; CFDS Department, Harwell U.K., Reference Notes, 2002;
- [9] Conybear J. G.: High-pressure gas quenching; *Advanced Materials & Processes*, Feb. 1993, pp. 20-21;
- [10] Herring D.H., Houghton R.L.: The Influence of Process Variables on Vacuum Carburizing; *Proc. of the 2<sup>nd</sup> Int. Conf. Carburizing and Nitriding with Atmospheres*, Cleveland, 1995, pp. 103-108;
- [11] Laumen Ch., Holm T., Lübben Th., Hoffmann E., Mayr P.: High-pressure gas quenching with hydrogen; *HTM – Haertere-Technische Mitteilung*, e Mar-Apr 1998, pp. 77-80;
- [12] Edenhofer B., Bouwman J.W.: Influence of furnace type and load size on the heat transfer coefficient of gas quenching; *HTM – Haertere-Technische Mitteilungen*, Mar-Apr 1998, pp. 102-107;
- [13] Preisser F., Seemann W., Zenker R.: Vacuum Carburizing with High Pressure Gas Quenching – The Application; *Proc. of the 1st International Automotive Heat Treating Conference*, Puerto Vallarta, Mexico, 1998, pp. 135-147;
- [14] Preisser F., Seemann W., Zenker R.: Vacuum Carburizing with High Pressure Gas Quenching – The Process; *Proc. of the 1st International Automotive Heat Treating Conference*, Puerto Vallarta, Mexico, 1998, pp. 142-148;
- [15] Hoffmann F. T., Lübben T., Mayr P.: Innovations in Quenching Systems and Equipment: Current Status and Future Developments; *Heat Treatment of Metals*, 1999, pp. 63-67;
- [16] Lübben T., Hoffmann F., Mayr P., Laumen Ch.: Gas Quenching: Influence of Diameter and Heat Transfer Coefficient on Hardness for different Steel Grades; *Proc. 3<sup>rd</sup> Int. Conference on Quenching and Control of Distortion*, 1999, Prague, ASM Int., pp. 83-92;
- [17] Kula P.: Nawęglanie próżniowe: technologia, ekonomia urządzenia; *Materiały seminarium szkoleniowego*, SECO/WARWICK, Ed. IV; Świebodzin, Poland, 2000;
- [18] Górecki M., Jasiński P.: Symulacja komputerowa zagadnień cieplno-przepływowych przy utwardzaniu otworów; *XVIII Zjazd Termodynamików*; Warszawa 2002, pp. 505-512;
- [19] Kula P., Olejnik J., Kowalewski J.: FineCarb™ - the smart system for vacuum carburizing. *Bulletin SECO/WARWICK*, 9/2003;
- [20] Lübben T., Hoffmann F., Mayr P., Laumen Ch.: The Uniformity of Cooling in High-pressure Gas Quenching; *Heat Treatment of Metals*, 2003, pp. 57-61;
- [21] Elkhatatny I., Morsi Y., Blicblau A. S., Das S., Doyle E. D.: Numerical analysis and experimental validation of high pressure gas quenching; *Int. Journal of Thermal Sciences*, Vol. 42. April 2003, pp. 417-423.;
- [22] Jasiński P., Fodemski T.: Analiza zjawisk cieplnych podczas hartowania części maszyn w strudze gazu, oparta na symulacji komputerowej; *XII Symp. Wymiany Ciepła i Masy*, AGH-Kraków, 2004, Vol. 1, pp. 365-377.